09

Correction of the GN model for fiber optical communication links with distributed Raman amplification

© D.D. Starykh,[1] L.A. Samodelkin,[1,2] O.E. Nany,[1,2] V.N. Treshchikov[1]

[1] Research and Development Center T8,
107076 Moscow, Russia
[2] Moscow State University,
119991 Moscow, Russia
e-mail: starykh@t8.ru

Received May 15, 2023
Revised July 30, 2023
Accepted August 31, 2023

Novel method of nonlinear interchannel distortions generation in coherent multichannel fiber-optic transmission was proposed. Series of experiments was made to measure nonlinear interference noise in links with distributed amplification by co-propagating Raman pump. Based on the measurement results, a correction term to known GN-model formulas for calculating the power of nonlinear interference noise was proposed. Proposed formula demonstrate acceptable accuracy.

Keywords: Coherent communications, distributed Raman amplification, unrepeatered transmission, GN model, nonlinear interference.

DOI: 10.61011/TP.2023.11.57504.123-23

Introduction

To date, coherent data transmission via fiber-optic communication lines (networks) (FOCL) has been the most powerful method for fast signal long-distance transmission [1]. Multiple long and extra long fiber spans more than 140 km in length are one of the features of optical network construction in Russia. To ensure signal transmission without significant impairment, counter- and co-pumped Raman amplifiers are used for these network sections [2–4].

For coherent-channel communication network simulation, a series of models was developed [5–10] that facilitate simplified description of some nonlinear effects without numerical solution of nonlinear propagation equations [11] that require long-term computation with necessary accuracy. An additive Gaussian noise model described in detail in [10] (hereinafter referred to as — GN-NLI (Gaussian Noise NonLinear Interference)) is the most common. The next step in the development of this model was the generation of approximation equations described in [12] to ensure considerable acceleration of computation without degradation of accuracy.

The model described in the fundamental paper [10] included a set of restrictions that made the scope of application narrower. In particular, the authors pointed out that the model was not applicable to distributed amplification lines [13] that prevented simulation of extra-long spav lines. Some more recent studies attempted to extend the scope of application of the GN-NLI to the distributed amplification case. For example, in [14], the authors proved that this model is applicable to distributed amplification lines due to counter distributed Raman amplification (counter-DRA), however, this case in not interesting for practical applications, because counter pumping is used at the fiber span end where the signal power is low and nonlinear distortions are negligibly low. In [15], the authors considered interlink Raman amplification that slightly changes the longitudinal signal power profile. However, the most complicated case of co-pumped distributed Raman amplification (co-DRA) has not been addressed in the previous literature.

The objective of the study was to extend the scope of application of the GN-NLI model to the co-pumped distributed Raman amplification case. The first steps in this area were made by us in [16], where a phenomenological model of non-linear internal coherent link distortions in co-DRA conditions was offered. This study has performed experimental investigations of intralink and interlink distortions that were used to offer the GN-NLI model modification that extended the scope of application.

1. Theory

GN−NLI is based on the approximated solution of the nonlinear Schrödinger equation (NSE) using the small perturbation theory. Several base assumptions were made to derive this solution:

- perturbation from nonlinear effects was low compared with the signal;
- signal is a random process with normal distribution;
- non-linear perturbation may be described as the additive Gaussian noise.

Strictly speaking, all three base assumptions may not be fulfilled in real FOCL. However, the experimental investigations have shown that the derived equations are resistant to breach of base assumptions.

The approximate solution of NSE in [10] derived equation (1) for calculation of the spectral power density (SPD) of nonlinear interference noise (NIN).

$$G_{NL}^{GNRF}(f)=\frac{16}{27}\gamma^2\int_{-\infty}^{\infty}\int_{-\infty}^{\infty}G_{TX}(f_1)G_{TX}(f_2)G_{TX}(f_1+f_2-f)$$

$$\times\left|\int_0^{L_s}L_{\text{eff}}e^{j4\pi^2(f_1-f)(f_2-f)\beta_2 z}dz\right|\chi(f_1,f_2,f)df_1df_2, \quad (1)$$

where γ is the fiber nonlinearity factor; G_{TX} is the spectral power density of a multichannel signal; L_{eff} is the effective fiber length depending on the longitudinal signal power distribution; χ — is the term responsible for efficient interference of nonlinear noise induced in various FOCL spans (for a single-span line $\chi=1$); f_1, f_2 — are the frequencies used for integration; β_2 — is the dispersion factor; L_S is the fiber span length.

Equation (1) calculates the accurate nonlinear interference noise spectrum. However, to achieve the required computational accuracy of the nonlinear signal-to-noise ratio of 1 dB in numerical evaluation of the volume integral (1), a dense frequency grid with a step not less than 0.1 GHz shall be used. However, computation of even a small number of channels (up to ten) requires several computing time hours. In real practice, FOCL design requires repeated solution of the signal power optimization problem and, therefore, nonlinear distortion computation, and the total optimization time shall not exceed several minutes. Taking this into account, approximate equation (2) was offered in [12] to calculate NIN SPD only in the center of the channel under test (CUT).

$$G_{NL}^{GNCFF-2019}=\frac{8}{27}\frac{\gamma^2}{\pi}G_{\text{GUT}}\times\ldots$$

$$\ldots\times\left[G_{\text{GUT}}^2\frac{a\sinh\left(\frac{\pi^2}{2}\frac{|\beta_2^{\text{GUT}}|}{\alpha_{\text{CUT}}}B_{\text{GUT}}^2\right)}{|\beta_2^{\text{GUT}}|\alpha_{\text{GUT}}}+\ldots\right.$$

$$\left.\ldots+2\sum_n G_n^2\frac{a\sinh\left(\pi^2\frac{|\beta_2^n|}{\alpha_n}\left[f_n-f_{\text{GUT}}+\frac{B_n}{2}\right]B_{\text{GUT}}\right)-a\sinh\left(\pi^2\frac{|\beta_2^n|}{\alpha_n}\left[f_n-f_{\text{CUT}}-\frac{B_n}{2}\right]B_{\text{CUT}}\right)}{2|\beta_2^n|\alpha_n}\right], \quad (2)$$

where G_{GUT} is SPD of the channel under test on the assumption of the Nyquist spectrum profile; β_2^{GUT} is the dispersion factor at the carrier frequency of the channel under test; α_{CUT} — is the linear attenuation factor at the carrier frequency of the channel under test; B_{CUT} — is the spectrum width of the channel under test; G_n — is SPD of one nth affecting channel; β_2^n is the dispersion factor at the carrier frequency of then$n$th affecting channel; α_n — is the linear attenuation factor at the carrier frequency of the nth affecting channel; B_n is the spectrum width of the nth affecting channel; f_{CUT} is the carrier frequency of the channel under test; f_n is the carrier frequency of the nth affecting channel.

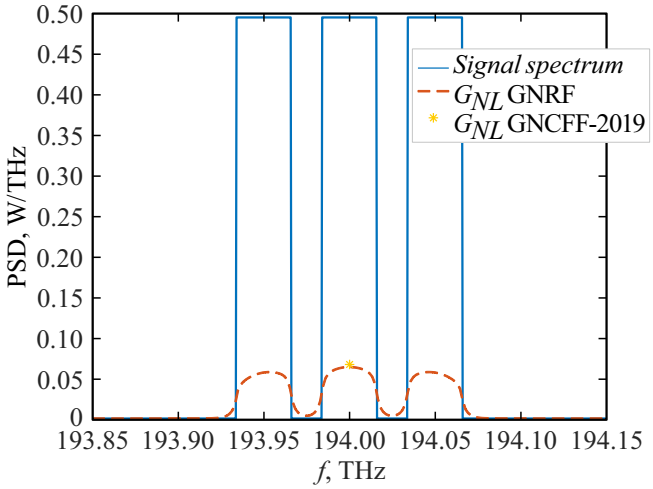

Figure 1. Example of nonlinear interference noise analysis (orange line (online version)) for three rectangular spectrum channels (blue line (online version)). For comparison, calculation of the spectral power density of noise in the center of the channel using an approximate equation (star) is given.

Let's consider the use of above equations for NIN SPD calculation. Example of the spectral power density calculated for a group of three rectangular spectrum channels is shown in Figure 1. As shown in the Figure, NIN SPD depends on frequency. In addition, it is shown that approximate equation (2) in the center of the CUT band gives the result that coincides with the accurate SPD value calculated using equation (1). By making a conservative assumption that NIN SPD is the same throughout the signal band, full NIN power coming to the receiver may be estimated. The error of this approximate approach is about 1 dB when calculating the NIN power. This error is acceptable, because, when signal power is set to achieve the maximum margin of OSNR (Optical Signal-to-Noise-Ratio) in the line, the nonlinear noise power is usually equal to maximum 1/3 of the total optical noise [17], therefore the impact of this effect on the estimation accuracy of the final system performance is much lower than 1 dB.

Optical signal transmission performance is certainly associated with the full optical signal-to-noise ratio OSNR_Σ [18]. Inverse of OSNR_Σ is a full noise power normalized to the signal power. As shown in [17], the inverse of OSNR_Σ may be calculated as a sum of inverse signal-to-noise ratios induced by noise of various origin:

$$\frac{1}{OSNR_\Sigma}=\sum_i\frac{1}{OSNR_i}. \quad (3)$$

amplified spontaneous emission noise (ASE noise) and the related signal-to-noise ratio OSNR_{ASE} are the main source of noise in optical communication systems. In the nonlinear noise model, nonlinear signal distortions are approximately described by the additive Gaussian noise and

related signal-to-noise ratio $OSNR_{NL}$. Relation between NIN SPD and $OSNR_{NL}$ is described by equation

$$OSNR_{NL} = \frac{P_S}{P_{NL}} = \frac{P_S}{G_{NL} \times BW_{ref}}, \quad (4)$$

where P_S is the full signal power, P_{NL} is the NIN power in the 12.5 GHz reference band, G_{NL} is NIN SPD in the signal band, BW_{ref} is the reference band width in Hz.

The proposed equations for nonlinear signal-to-noise ratio may be used for communication line analysis using the mathematical tools described in [17]. However, it should be noted that the highlighted noise behavior, filtration in the coherent receipt circuit and the features of the phase distortion compensation algorithms in digital signal processors may result in the situation when the identical nonlinear noise level coming to the channeling equipment receiver may impair the reception quality in various degrees for various coherent transceiver models. To consider this effect, direct experiments are carried out to assess the nonlinear distortion effect on the reception quality, and the correction factor is calculated using equation (2).

It should be noted that it is shown in [12] that equation (2) is not intended to be used in communication lines with longitudinal amplification distribution. However, as will be shown below, if the effective length parameter is redefined and definition (6) is used instead of original equation (5), then equation (2) in [12] with the corresponding corrective terms may be successfully used to calculate nonlinear distortions in the co-pumped Raman amplification lines. It should be noted that, when there is no longitudinal amplification in the communication fiber and the span length considerably exceeds the effective length, equation (6) changes to equation (5):

$$L_{\text{eff},a} = \frac{1}{\alpha}, \quad (5)$$

$$L_{\text{eff}} = \int_0^L \frac{P_S(z)}{P_S(0)} dz, \quad (6)$$

where $P_S(z)$ is the longitudinal signal power profile in fiber, this quantity may be found by solution rate equations describing the Raman amplification [19]; L is the fiber length.

The review of studies devoted to simulation of nonlinear distortions in coherent communication systems shows that the additive Gaussian noise may be used for FOCL design. However, the original model needs adjustment for the simulation of FOCL containing co-pumped distributed Raman amplifiers. For this purpose, experimental investigations were carried out to find corresponding corrective terms for the original equation and to expand its scope of application.

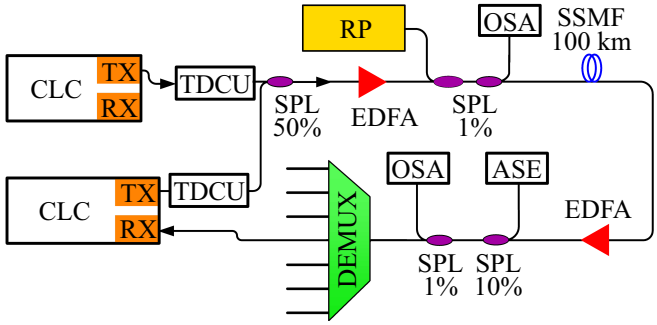

Figure 2. Experimental setup intended to generate the affecting channels using the real channeling equipment and tunable dispersion compensation units (TDCU).

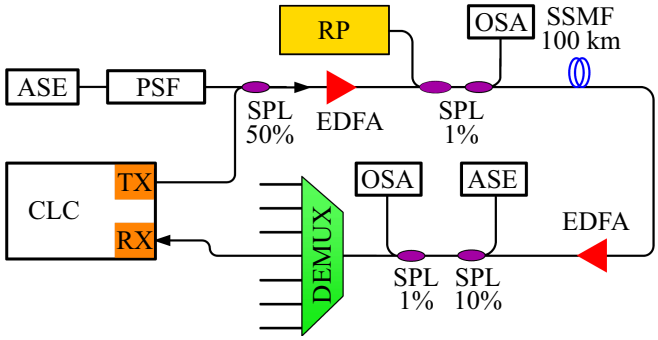

Figure 3. Experimental setup intended to generate an arbitrary number of affecting channels using the filtered amplified spontaneous luminescence noise.

2. Nonlinear distortion measurement procedure

For NIN measurement, differential measurement procedures have been developed and successfully used repeatedly on the basis of signal quality comparison with or without any nonlinear distortion. The theory describing these procedures for intralink and interlink distortion measurements is describe in detail in [20–22].

The setup shown in Figure 2 uses real coherent channeling equipment and tunable chromatic dispersion compensation unit as the affecting emission. Such type of experimental setup is traditionally used to measure nonlinear distortions occurring in the fiber optic path [22]. It should be noted that this setup has a considerable disadvantage: to measure the effect of several coherent channels, the number of expensive coherent transceivers (CLC) shall be increased, which limits the list of available study scenarios.

To expand the scope of study, an alternative method was offered for formation of the affecting channels using the amplified spontaneous luminescence (ASE) source and software-triggered filter (PSF). This type of affecting emission is hereinafter referred to as the „channeled noise illumination“ (CNI). The setup layout is shown in Figure 3.

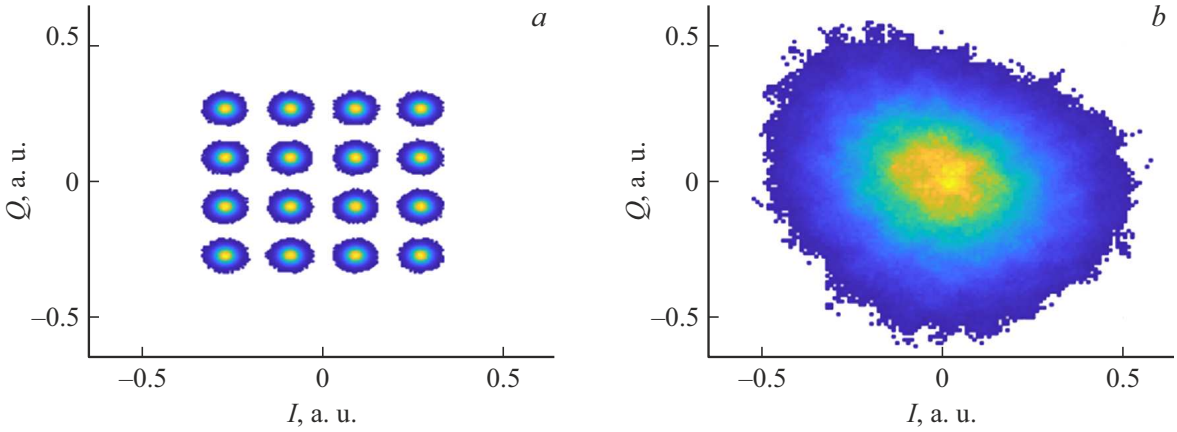

Figure 4. Standardized phase diagrams of a signal at the QAM receiver output (*a*) and 100 km SSMF fiber output (*b*).

Using both setups, it was experimentally shown that CNI induces cross-link nonlinear perturbation corresponding to coherent communication channel with high accumulated dispersion and similar spectrum profile. As will be shown in Section 3, cross-link effect increases with accumulation of the residual dispersion in the affecting channel. Therefore, the CUT signal quality measurement using CNI provides conservative estimation of the cross-link effect of adjacent coherent channels to build a conservative model of nonlinear distortions on the basis of the measurements.

Using CNI, a group of affecting channels was simulated, these channels were combined with the coherent channel under test (CLC), via which the signal with DP-QPSK modulation format and a symbol rate of35 Gbaud was transmitted, using an optical combiner (SPL). Then the group signal was gradually amplified using and erbium doped fiber amplifier (EDFA) and co-pumped distributed Raman amplifier (RP — Raman Pump). The distributed amplification took place in the G.652D single-mode optical fiber at whose output the fiber-attenuated signal was re-amplified by the erbium amplifier and mixed with the amplified spontaneous luminescence noise (ASE). The ASE noise must be added to enable using the differential nonlinear noise measurement procedure. The fundamental idea of the differential method is in the bit error rate (BER) measurement in the signal received by the coherent transmitting-and-receiving equipment with and without nonlinear distortions. Then the known [23] dependences of BER on signal-to-noise ratio (SNR) are used to restore the nonlinear noise power that is added to the noise from other sources present in both measurements. However, to ensure reliable measurement of BER and, accordingly, of SNR, values of the former shall be quite high in both scenarios (higher than 10^{-5}), for this, the additional ASE noise is added to the received signal.

3. Accumulated chromatic dispersion effect

This Section is focused on justification of replacement of the phase-modulated channel with the channel model formed by the filtered ASE noise. As mentioned above, the assumption that the coherent channel may be treated as a random normal distribution process is one of the GN model fundamentals. However, for this assumption to become true, quite high non-compensated dispersion shall be accumulated in the channel. As shown by the absence of radial symmetry of the phase signal diagram in Figure 4, the transmitter output signal field, even after hundreds of kilometers of the communication fiber, cannot be represented as a process with identical normal distribution in both quadratures.

This divergence from the basic prerequisite results in high overestimate of the nonlinear noise in short communication lines. It should be noted that this effect is valid both for the intralink and interlink interaction.

Dependence of the intralink distortions on the accumulated dispersion in the channel under test has been first demonstrated in [24], the comprehensive description of the effect considering the longitudinal amplification case was offered in [16]. The general view of this dependence is shown in Figure 5. Position and depth of the curve valley depend on the type of fiber, electronic dispersion pre-compensation in the channel and modulation format.

Interlink nonlinear distortions depend simultaneously on the accumulated dispersions in the channel under test and affecting channel. Similar 2D dependence was measured herein, the result is shown in Figure 6.

As shown in Figure 6, the 2D dependence on the accumulated dispersion has a „double saddle“ shape. Interlink interaction is minimum at zero accumulated dispersion, grows steadily and achieves its constant value with the increase in the accumulated dispersion in the affecting channel. This effect may be explained by the fact that, as known from [25], the phase cross-modulation depends

on the power modulation depth of the affecting emission. Therefore, the initially phase-modulated channel exerts a low nonlinear impact on CUT, however, when the non-compensated dispersion in the affecting channel increases, the phase modulation transforms into the amplitude modulation [26] resulting in the increase in interlink nonlinear distortions. It should be noted that the dependence of the interlink interaction on dispersion accumulated in CUT is inverse: interlink nonlinear impact is maximum at the minimum dispersion and decreases steadily when the plateau is achieved with dispersion growth in the channel. This effect is a bit more complicated than the previous one and is associated simultaneously with the emission propagation physics in the fiber and operational aspects of phase distortion compensation algorithms in the coherent receiving-and-transmitting equipment. Under the dispersion, the CUT pulse widths increase and, thus, phase distortions into each individual pulse are introduced by multiple affecting channel pulses that are propagated at another rate and may have a lower width. Since the communication signal is close to the random process, nonlinear phase distortions of various pulses are not correlated and partly compensate each other. Thus, when processed digitally, a signal previously subjected to digital dispersion compensation has on average lower phase distortions that are more easily compensated by the phase compensation algorithms.

Figure 6 also shows similar dependences of the interlink distortions on dispersion when the real coherent affecting channel is replaced with a channel formed from by the tunable ASE noise filter. According to the diagram, when the accumulated dispersion is high, the impact of the DP-QPSK modulation channel approaches the impact of the channel formed by the ASE noise filter. the effect is caused by the repeated phase-to-amplitude modulation conversion, and vice versa, and, thus, the phase-modulated signal is converted into a random Gaussian process equivalent to the amplified spontaneous luminescence.

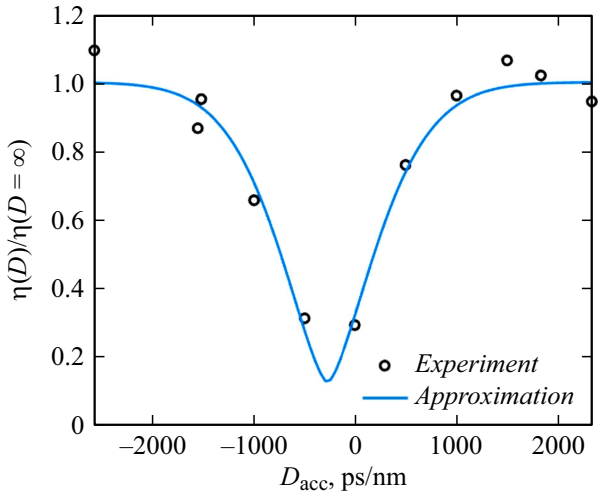

Figure 5. Standardized dependence of the nonlinear factor describing the intralink distortions on the accumulated dispersion.

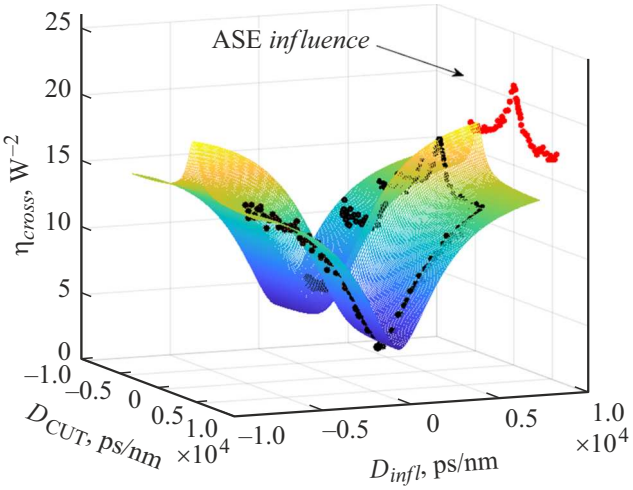

Figure 6. experimentally measured dependence of the interlink nonlinear factor on the accumulated dispersion in the coherent channel under test (D_{CUT}) and the affecting coherent channel (D_{infl}) (marked with black dots), and experimental data approximation.

Therefore, for further experimental investigations of cross-link nonlinear interaction, the authors generated the multi-channel affecting emission using CNI, while the dispersion accumulated in CUT at the fiber input was close to zero. This approach extended the list of the channel configurations under test and provided conservative estimate of the interlink nonlinear distortions.

As shown in Figure 6, in case of single-span FOCL with zero accumulated dispersion at the input, the above approach overestimates the nonlinear cross-link distortions by a factor of 3 to 3.5 on average. However, the overestimate in the multispan communication line will decrease to 25% already in the second fiber span due to the accumulated dispersion. In the multispan communication line, nonlinear noise from various spans are summarized, thus, the cross-link effect overestimate in a medium length (about 10 spans) communication line will approach 25%. To assess the full influence of this error, it should be taken into account that nonlinear noise accounts for less than 1/3 of the full noise power at finely tuned equipment settings. Thus, the nonlinear distortion overestimate will result in the transmission performance underestimate by max.10−15% which is acceptable for practical application of the model.

4. Experimental investigation findings

The experimental study measured the dependences of the nonlinear noise on the amplification factor of the co-pumped Raman amplifier (from 0 to 20 dB) with varying number of affecting channels from 0 to 40. Moreover, measurements were carried out for two standard interlink intervals of 50 GHz and 100 GHz. This measurement grid allowed to cover all main coherent channel and co-pumped Raman amplifier sharing scenarios.

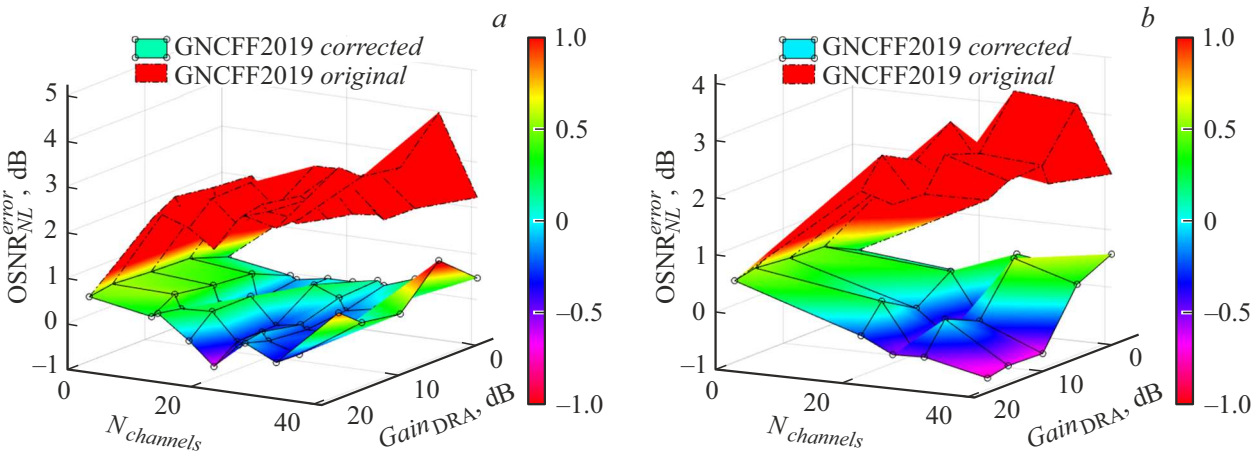

Figure 7. Dependences of the maximum difference between the calculated and measured nonlinear signal-to-noise ratio on the experiment conditions — number of channels and amplification factor of the co-pumped Raman amplifier for 50 (*a*) and100 GHz (*b*) two-frequency grids.

Curves on Figure 7 shows differences of nonlinear signal-to-noise ratios measured experimentally and calculated using the original and adjusted equations. It is shown that original equation (2) estimates the interlink nonlinear distortions with good accuracy (the number of affecting channels is equal to zero) at all amplification factors of the co-pumped Raman amplifier. However, when the number of affecting channels is increased, the divergence is increasing and achieves several decibels which is critical for FOCL simulation.

In order to use the above equation for nonlinearity assessment in the distributed amplification communication fiber lines, the effective length calculated using equation (6) was explicitly introduced in equation (2). In addition, to reduce the original dependence divergence from the experiment, a correction term was selected. The resulting corrected equations are written as follows:

$$G^{\mathrm{CUT}}_{NL\,2019corr} = \frac{8}{27}\frac{\gamma^2}{\pi}G_{\mathrm{CUT}} \times \ldots$$

$$\ldots \times \left[G^2_{\mathrm{CUT}}(L^{\mathrm{CUT}}_{\mathrm{eff}})^2 \frac{a\sinh\left(\frac{\pi^2}{2}|\beta_2^{\mathrm{CUT}}|L_{\mathrm{eff},a}B^2_{\mathrm{CUT}}\right)}{|\beta_2^{\mathrm{CUT}}|L^{\mathrm{CUT}}_{\mathrm{eff},a}} + \ldots \right.$$

$$\ldots + 2\sum_n f_{adj}(f_n - f_{\mathrm{CUT}}) \times G_n^2(L^n_{\mathrm{eff}})^2 \times \ldots$$

$$\left. \ldots \times \frac{a\sinh\left(\pi^2|\beta_2^n|L_{\mathrm{eff},a}\left[f_n - f_{\mathrm{GUT}} + \frac{B_n}{2}\right]B_{\mathrm{GUT}}\right) - a\sinh\left(\pi^2|\beta_2^n|L_{\mathrm{eff},a}\left[f_n - f_{\mathrm{CUT}} - \frac{B_n}{2}\right]B_{\mathrm{CUT}}\right)}{|\beta_2^n|L^n_{\mathrm{eff},a}} \right], \quad (7)$$

where $L^{\mathrm{CUT}}_{\mathrm{eff}}$ is the effective fiber length at the CUT carrier frequency; $L^{\mathrm{CUT}}_{\mathrm{eff},a}$ — is the asymptotic effective fiber length at the CUT carrier frequency, L^n_{eff} is the effective fiber length at the carrier frequency of the *n*th affecting channel, $L^n_{\mathrm{eff},a}$ is the asymptotic effective fiber length at the carrier frequency of the *n*th affecting channel,

$$f_{adj}(f_{n_{ch}} - f_{CUT}) = 0.65 \times \left[NoRaman + WithRaman \times \frac{10}{\sqrt{f^{GHz}_{n_{ch}} - f^{GHz}_{CUT}}} \right], \quad (8)$$

where *NoRaman* variable is equal to 1 without longitudinal co-pumping amplification and is equal to zero with longitudinal co-pumping amplification; *WithRaman* variable is equal to zero without longitudinal co-pumping amplification and is equal to 1 with longitudinal co-pumping amplification.

According to the curves in Figure 7, the corrected equation provides the assessment of non-linear distortions with minor error (max. 1 dB) that does not depend on the number of channels in the line.

Conclusion

Nonlinear distortions occurring in the FOCL coherent communication channels with co-pumped distributed Raman amplification have been investigated experimentally. The dependence of nonlinear intralink and interlink distortions on chromatic dispersion accumulated in affecting channel and channel under test has been obtained experimentall. It has been shown that the „channeled“ spontaneous luminescence noise with the power spectrum close to the spectrum of the affecting DP-QPSK channel with higher accumulated dispersion exerted nonlinear impact on CUT with a similar value. On the basis of the study, a measurement procedure has been proposed to simulate effecting channels with various symbol rate using the ASE noise source and programmable optical filter.

using the experimental findings,correction of the existing approximate GN model equation has been offered to extent the scope of application in the distributed amplification

communication line, including the communication line with co-pumped Raman amplifiers.

Conflict of interest

The authors declare that they have no conflict of interest.

References

[1] E. Agrell, M. Karlsson. J. Light. Technol., **27** (22), 5115 (2009). DOI: 10.1109/JLT.2009.2029064

[2] V. Gainov, N. Gurkin, S. Lukinih, S. Makovejs, S. Akopov, S. Ten, O. Nanii, V. Treshchikov, M. Sleptsov. Opt. Express, **22**, 22308 (2014). DOI: 10.1364/OE.22.022308

[3] D. Starykh, S. Akopov, D. Kharasov, V. Konyshev, S. Makovejs, O. Nanii, I. Shikhaliev, V. Treshchikov. IEEE Photon. Technol. Lett., **31** (22), 1799 (2019). DOI: 10.1109/LPT.2019.2947760

[4] S. Etienne, H. Bissessur, C. Bastide, D. Mongardien. In Eur. Conf. Opt. Commun. ECOC (2015). DOI: 10.1109/ECOC.2015.7341877

[5] H. Louchet, A. Hodžić, K. Petermann. IEEE Photon. Technol. Lett., **15** (9), 1219 (2003). DOI: 10.1109/LPT.2003.816133

[6] M. Nazarathy, J. Khurgin, R. Weidenfeld, Y. Meiman, P. Cho, R. Noe, I. Shpantzer, V. Karagodsky. Opt. Express, **16** (20), 15777 (2008). DOI: 10.1364/oe.16.015777

[7] W. Shieh, X. Chen. IEEE Photon. J., **3** (2), 158 (2011). DOI: 10.1109/JPHOT.2011.2112342

[8] A. Carena, V. Curri, G. Bosco, P. Poggiolini, F. Forghieri. J. Light. Technol., **30**, 1524 (2012). DOI: 10.1109/JLT.2012.2189198

[9] V.A. Konyshev, A.V. Leonov, O.E. Nanii, V.N. Treshchikov, R.R. Ubaydullaev. Opt. Commun., **355**, 279 (2015). DOI: 10.1016/j.optcom.2015.06.048

[10] P. Poggiolini, G. Bosco, A. Carena, V. Curri, Y. Jiang, F. Forghieri. J. Light. Technol., **32**, 694 (2014). DOI: 10.1109/JLT.2013.2295208

[11] G.P. Agrawal. Nonlinear Fiber Optics (Academic Press, 2019), DOI: 10.1016/C2018-0-01168-8

[12] P. Poggiolini, M.R. Zefreh, G. Bosco, F. Forghieri, S. Piciaccia. *OSA Technical Digest* (Optica Publishing Group, 2019), paper M1I.4 (2019). DOI: 10.1364/ofc.2019.m1i.4

[13] J. Bromage. J. Light. Technol., **22** (1), 79 (2004). DOI: 10.1109/JLT.2003.822828

[14] V. Curri, A. Carena, P. Poggiolini, G. Bosco, F. Forghieri. Opt. Express, **21** (3), 3308 (2013). DOI: 10.1364/oe.21.003308

[15] D. Semrau, R.I. Killey, P. Bayvel. J. Light. Technol., **37** (9), 1924 (2019). DOI: 10.1109/JLT.2019.2895237

[16] D.D. Starykh, I.I. Shikhaliev, V.A. Konyshev, O.E. Nanii, V.N. Treshchikov, R.R. Ubaydullaev, D.R. Kharasov. Quant. Electron., **48** (8), 767 (2018). DOI: 10.1070/QEL16685

[17] V.A. Konyshev, A.V. Leonov, O.E. Nanii, A.G. Novikov, V.N. Treshikov, R.R. Ubaydullaev. Quant. Electron., **46**, 1121 (2016). DOI: 10.1070/QEL16219

[18] W. Freude, R. Schmogrow, B. Nebendahl, M. Winter, A. Josten, D. Hillerkuss, S. Koenig, J. Meyer, M. Dreschmann, M. Huebner, C. Koos, J. Becker, J. Leuthold. In Int. Conf. Transparent Opt. Networks (2012). DOI: 10.1109/ICTON.2012.6254380

[19] C. Headley, G.P. Agrawal. *Raman Amplification in Fiber Optical Communication Systems* (Academic Press, 2005), DOI: 10.1016/B978-0-12-044506-6.X5000-2

[20] N.V. Gurkin, O.E. Nanii, A.G. Novikov, S.O. Plaksin, V.N. Treshchikov, R.R. Ubaidullaev. Quant. Electron., **43** (6), 550 (2018). DOI: 10.1070/QE2013v043n06ABEH015014

[21] D. Starykh, L. Samodelkin, A. Dorozhkin, O. Nany, V. Treshchikov, A. Vasiliev. LAST MILE Russ., **93**, 34 (2021). DOI: 10.22184/2070-8963.2021.93.1.34.38

[22] D.D. Starykh, L.A. Samodelkin, O.E. Nany, V.N. Trashchikov. Kvant. elektron., **52**, 934 (2022) (in Russian).

[23] E. Ip, A.P.T. Lau, D.J.F. Barros, J.M. Kahn. Opt. Express, **16**, 753 (2008). DOI: 10.1364/oe.16.000753

[24] V.A. Konyshev, A.V. Leonov, O.E. Nanii, A.G. Novikov, V.N. Treshchikov, R.R. Ubaydullaev. Opt. Commun., **349**, 19 (2015). DOI: 10.1016/j.optcom.2015.03.041

[25] J. Wang, K. Petermann. J. Light. Technol., **10** (1), 96 (1992). DOI: 10.1109/50.108743

[26] U. Gliese, S. Norskov, T.N. Nielsen. IEEE Trans. Microw. Theory Tech., **44**, 1716 (1996). DOI: 10.1109/22.538964

Translated by Ego Translating